Journal of Applied Mechanics Vol. 6, pp. 1227-1234 (August 2003) JSCE

Fatigue damage analysis of welded structural members by using damage mechanics

Khampaseuth Thepvongsa*, Yoshimi Sonoda** & Hiroshi Hikosaka***

*Graduate student of Eng., Dept. of Civil Eng., Kyushu University, 10-1, Hakosaki 6, Higashi-ku, Fukuoka 812-8581
**Dr. of Eng., Assoc. Professor, Dept. of Civil Eng., Kyushu University, 10-1, Hakosaki 6, Higashi-ku, Fukuoka 812-8581
**Dr. of Eng., Professor, Dept. of Civil Eng., Kyushu University, 10-1, Hakosaki 6, Higashi-ku, Fukuoka 812-8581

The fatigue damage analysis of welded structural members based on continuum damage mechanics is carried out. For high cycle fatigue, plastic deformation and damage occurs at the micro-scale and it is difficult to evaluate it by the macro behavior. Therefore, a two-scale model presented by Lemaitre is introduced to evaluate the damage evolution. In this study, to determine the material parameters for damage evolution at the micro-scale, the identification method is proposed, and confirmed the validity of this procedure. In order to consider the effect of residual stress on fatigue behavior of welded joints, the inherent strain method is also applied to this analysis. It is confirmed that the proposed method could give the reliable fatigue lifetime of welded structural members.
Key Words: high cycle fatigue, welded structure, continuum damage mechanics.

1. Introduction

Decision concerning the maintenance and replacement of the existing bridges gives serious impact on the traffic patterns and economy of the surrounding community. Thus, extending the lifetime of bridge structures plays an important role in reducing the total life cycle costs. Therefore, it is necessary to evaluate the durability and lifetime of bridge structures accurately. In case of steel bridge, structures are commonly fabricated by welding. These welded structures are often subjected to high cyclic loading and subsequently failures may occur due to fatigue damage at the welded joints[1) 2)]. The lifetime of welded structures subjected to cyclic loading, consists of two phases: crack initiation and crack propagation to final failure. The problem of crack propagation up to failure of structures has received much attention through development of fracture mechanics[3)]. In this framework, the assumption of a pre-existing crack is required to estimate the growth of a crack through the final failure. However, it is difficult to assume the pre-existing crack size in advance. Thus, an effective procedure for life prediction of welded structures based on the continuum damage mechanics (CDM)[4)] is proposed. CDM could describe both crack initiation and propagation in multi-axial loading condition with appropriate failure criteria. For high cycle fatigue (HCF), materials do not exhibit such a macroscopic plasticity and damageable behavior. However, it is considered that plastic deformation and damage occur at microscopic scale. Therefore, a two-scale model presented by Lemaitre [4) 5)] is introduced to evaluate the damage evolution at the microscopic scale by using the law of localization of self-consistent scheme. As it is difficult to identify the parameters directly at the micro-scale from the material experiment, the identification method is proposed to obtain the reliable material parameters.

The fatigue damage behavior of welded joints is complicated by numerous factors with respect to welding condition. Residual stresses that exist in the welded joints could be regarded as the result of incompatible thermal strains. These residual stresses reduce the fatigue life of welded structures, particularly when a tensile residual stress exceeds yield stress at the weld toe regions[6)]. Therefore, the effect of residual stress on fatigue behavior of welded structures is considered in this analysis. In this study, the simplified prediction of residual stresses based on the inherent strain method [7) 8)] is carried out. The fatigue damage analysis of T-joint is demonstrated to clarify the accuracy of the proposed method. The analytical results are compared with experimental results to confirm the validity.

2. Fatigue Damage Analysis Procedure

The high cycle fatigue damage analysis and life prediction of welded structural members are performed by the following two steps: 1) The welding residual stresses are estimated by using the inherent strain method. 2) The fatigue damage analysis based on the continuum damage mechanics is carried out.

2.1 Determination of Residual Stresses

The residual stresses can be obtained by several experimental measuring methods. These methods can be classified into destructive and non-destructive methods. Furthermore, the thermal finite element analysis can also be applied to the simulation of welding process.

Although all the methods above based on measurements or thermal elastic-plastic analysis can give accurate results, it is time-consuming. Therefore, a simplified procedure for evaluating the residual stresses in thin walled structures is applied in this study. This method is based on the inherent strain method, which was proposed by Ueda and Yuan [7) 8)].

In this idea, considering the internal stress σ_{ij}^0 as residual stresses in the weldment. Then total strains ε_{ij} are evaluated by the sum of elastic strains ε_{ij}^e and inherent strains ε_{ij}^* as:

$$\varepsilon_{ij} = \varepsilon_{ij}^e + \varepsilon_{ij}^* \tag{1}$$

and the Hook's law is written as

$$\sigma_{ij}^0 = E_{ijkl}\varepsilon_{kl}^e = E_{ijkl}(\varepsilon_{kl} - \varepsilon_{kl}^*) \tag{2}$$

where E_{ijkl}: elastic modulus tensors.

The residual stresses σ_{ij}^0 are the self-equilibrium stresses with no existence of external forces, thus the force equilibrium condition yields

$$\sigma_{ij}^0 n_j = (E_{ijkl}\varepsilon_{kl})n_j - (E_{ijkl}\varepsilon_{kl}^*)n_j = 0$$

and

$$\sigma_{ij,j}^0 = (E_{ijkl}\varepsilon_{kl})_{,j} - (E_{ijkl}\varepsilon_{kl}^*)_{,j} = 0 \tag{3}$$

where n_j: unit normal vector.

If the inherent strains are given, the residual stresses can thus be evaluated by the elastic finite element method using the above equations. The simplified method to determine the inherent strains is given as the following procedure.

(1) Inherent strain in butt welds

The longitudinal inherent strain distribution in the transverse section of a butt weld can be approximated by a trapezoid as shown in Fig. 1 and Fig. 2a.

From the numerical studies, Ueda and Yuan[7)] established some formulas for description of the approximated distribution and magnitude: the peak value $\hat{\varepsilon}_x^*$, the width of inherent strains zone b and the width of heat-affected zone (HAZ) y_H. The formulas were derived for a butt joint in a plate with a width of $2B$ as follows, assuming that the heat source is applied simultaneously to the entire weld line (y=0), so that the material deforms uniformly in the direction perpendicular to the weld line[7)]

$$y_H = \frac{0.242Q}{c\rho(T_m - T_0)}$$

$$b = \xi b_0 \tag{4}$$

$$\hat{\varepsilon}_x^* = \zeta\hat{\varepsilon}_{x0}^*$$

and

$$b_0 = \frac{0.242\alpha EQ}{c\rho h\sigma_{YB}}$$

$$\hat{\varepsilon}_{x0}^* = \frac{\sigma_{YW}}{E} \tag{5}$$

$$\xi = 1 - \frac{0.27\alpha ET_{av}}{\sigma_{YB}}$$

$$\zeta = -1 - \frac{0.27\alpha ET_{av}}{\sigma_{YB}}$$

$$T_{av} = \frac{Q}{c\rho A}$$

where

Q: line heat input (J/mm)

T_m: mechanical melting point over which yield stresses disappear (°C)

T_0: room temperature(°C)

c: specific heat (J/g°C)

ρ: density(g/mm^3)

h: thickness of plate (mm)

α: linear thermal expansion coefficient(1/°C)

E: Young's modulus (GPa)

σ_{YW}: yield stress of weld metal and HAZ (MPa)

σ_{YB}: yield stress of base metal (MPa)

A: area of transverse cross section (mm^2)

A simple example of a residual stress distribution is shown in Fig. 2b. The magnitude of $\bar{\varepsilon}_x$ is found from the force equilibrium condition.

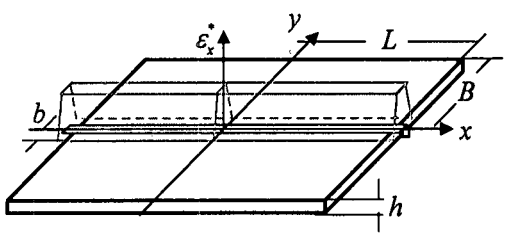

Fig. 1 Butt welded plate

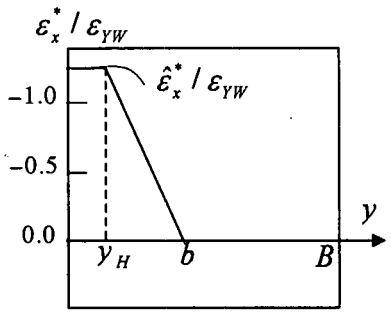

(a) inherent strain

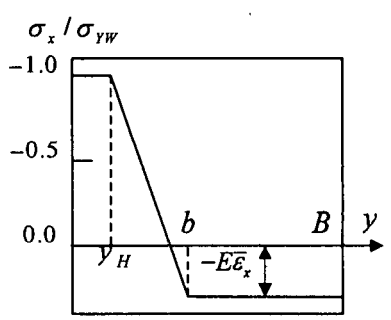

(b) residual stress

Fig. 2 Inherent strain and residual stress distributions

(2) Inherent strain in T-joints and I-joints

The formulas in the previous section can be applied to T-joints and I-joints with appropriate modifications[8)].

The magnitude of the inherent strain is practically the same for a butt weld and a T-joint. Thus, only the width of the inherent strain zone b has to be modified. The heat input in a T-joint is different from a butt joint. This effect can be taken into account by replacing the heat input Q by an equivalent heat input $Q'=2Qh/(2h_f+h_w)$ (see Fig. 3) and the value of b_0 is given by the following equation:

$$b_0 = \frac{0.484\alpha EQ}{c\rho(2h_f + h_w)\sigma_{YB}} \tag{6}$$

where h_w and h_f are the plate thickness of the web and the flange, respectively.

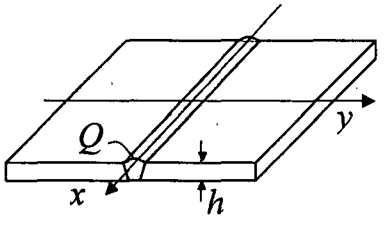

(a) butt weld

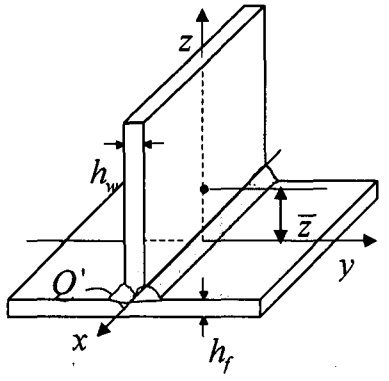

(b) T-joint

Fig. 3 Determination of equivalent heat input

In the case that the average temperature T_{av} rises (T_{av}>30°C), significant bending deformations may occur as a consequence of the uniform heat input in the web of the T-joint or I-joint. Therefore, a subsequent modification has to be made by dividing the longitudinal strain in the flange into two parts: one is due to the uniform deformation and the bending deformation. The effect of the uniform deformation can be evaluated by the formulas derived for a butt weld. The bending moment in the web is proportional to the average temperature in the whole section as:

$$M \approx \alpha E T_{av} A\bar{z} \tag{7}$$

where $\bar{z}$: distance between the weld center and the neutral axis of the transverse section.

The longitudinal strain can be calculated by beam theory as $\varepsilon'_x = \frac{M}{EI}\bar{z} \approx \alpha T_{av}\frac{A\bar{z}^2}{I}$; I is the moment inertia of the cross section. Thus, the bending part can be taken into account by increasing the average temperature as:

$$T'_{av} = T_{av} + \Delta T_{av} \approx (1+\phi)T_{av}$$
$$\phi = \bar{z}^2 A / I \tag{8}$$

hence

$$\xi = 1 - \frac{0.27\alpha E T_{av}(1+\phi)}{\sigma_{YB}} \tag{9}$$

Then the magnitude of longitudinal inherent strain in a T-joint can be evaluated by using Eqs. (4) and (5), while the distribution can be obtained by Eqs. (6) and (9). The inherent strain distribution in I-joint can also be evaluated by means of the same procedure.

2.2 Continuum Damage Mechanics

Material deterioration is an irreversible phenomenon during the damage evolution process, which may be interpreted as the growth of micro-defects and micro-cavities at the early state. The effect of these micro-defects is evaluated in the mesoscale plane that can be defined in a representative volume element (RVE)[4]. The damage variable is considered as the degree of degradation of material in the homogeneous field. Therefore, the basic image of damage variable D is defined as the loss of effective area in the meso-scale (RVE) (see Fig.4):

$$D = \frac{A_D}{A_0} \tag{10}$$

where A_0: the total area of considered plane, A_D: the area of all micro-defects.

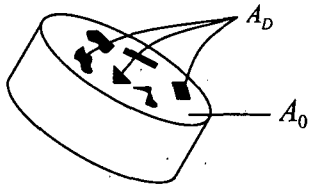

Fig. 4 Basic definition of damage variable

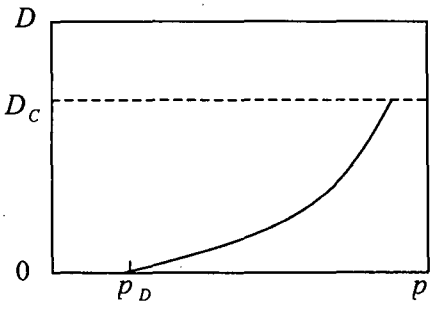

Fig. 5 Damage evolution

The damage evolution is derived from the associated flow rule with the strain energy density release rate Y and the existence of potential of dissipation F_D based on the thermodynamics framework. Then, it is assumed to be proportional to the increment of accumulated plastic strain. Thus, it is obtained directly by

$$dD = \frac{\partial F_D}{\partial Y} d\lambda = \left(\frac{Y}{S}\right)^n dp \tag{11}$$

where $d\lambda$ is the plastic multiplier, S *and* n are the damage energy strength and exponent of damage evolution, respectively.

The accumulated plastic strain caused by micro defects is defined as:

$$dp = \sqrt{\frac{2}{3} d\varepsilon_{ij}^{p} d\varepsilon_{ij}^{p}} \tag{12}$$

where dp and $d\varepsilon_{ij}^{p}$ are the accumulated plastic strain increment and plastic strain increments, respectively.

It is assumed that damage occurs when the accumulated plastic strain p reaches a certain value p_D. The subsequent damage growth up to rupture occurs at the meso-scale (macrocrack initiation), when damage variable reaches the critical value Dc (see Fig. 5). If the stored energy in an arbitrary stress state is the same as in the uniaxial tension, the damage threshold is determined

$$p_D = \varepsilon_{PD} \frac{(\sigma_u - \sigma_f)}{(\sigma_{eq} - \sigma_f)} \tag{13}$$

where σ_u, σ_f, σ_{eq} are the ultimate, fatigue limit and von Mises equivalent stresses, respectively; ε_{PD} is the damage threshold in pure tension. Notice that in Eq. (13) the initial yield stress is applied to the Mises equivalent stresses (σ_{eq}=σ_y=const) [4].

(1) Damage model for high cycle fatigue (Two-scale model)

When the amplitude of the loading is lower than the yield stress, the plastic strain cannot be observed at the mesoscale. Consequently, for high cycle fatigue, it is considered that damage and plasticity occur at the micro-scale. Therefore, the two-scale model is applied to evaluate the damage evolution in a weak micro-inclusion embedded in a RVE [5].

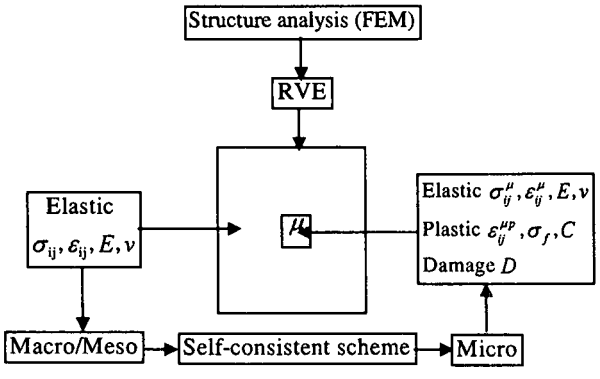

Fig. 6: Two-scale model, by Lemaitre [5]

It is considered that a meso-volume element is elastic everywhere except in a micro-volume inclusion μ under the elastoplastic state as shown in Fig. 6. The inclusion has the same properties as the meso-domain except for the plasticity threshold σ_y^{μ} (=σ_f; fatigue limit of the material).

The damage evolution law is now written in terms of microscopic fields as

$$\dot{D} = \left(\frac{Y^{\mu}}{S}\right)^{n} \dot{p}^{\mu} \tag{14}$$

The strain energy release rate Y^{μ}, taking into account the different behaviors in tension and compression, is written as

$$Y^{\mu} = \frac{1+\nu}{E}\left[\frac{\langle\sigma_{ij}^{\mu}\rangle\langle\sigma_{ij}^{\mu}\rangle}{(1-D)^2} + h\frac{\langle-\sigma_{ij}^{\mu}\rangle\langle-\sigma_{ij}^{\mu}\rangle}{(1-Dh)^2}\right] - \frac{\nu}{E}\left[\frac{\langle\sigma_{kk}^{\mu}\rangle^2}{(1-D)^2} + h\frac{\langle-\sigma_{kk}^{\mu}\rangle^2}{(1-Dh)^2}\right] \tag{15}$$

where h is the crack closure parameter (for most metal $h \approx 0.2$), and $\langle . \rangle$ means the positive part, i.e., $\langle x \rangle = x$ if $x > 0$, $\langle x \rangle = 0$ if $x \le 0$.

In order to perform the calculation by the macroscale response, the stresses at micro-scale σ_{ij}^{μ} are evaluated from the stresses at macroscale σ_{ij} by mean of the self-consistent scheme [5) 9)]:

$$\sigma_{ij}^{\mu} = \sigma_{ij} - aE\varepsilon_{ij}^{\mu p} \tag{16}$$

where a is given by Eshellby's analysis of a spherical inclusion [10],

$$a = \frac{(1-\beta)}{(1+\nu)}, \quad \beta = \frac{2(4-5\nu)}{15(1-\nu)} \tag{17}$$

where ν is Poisson's ratio.

The constitutive equations at the micro-scale that apply the kinematic hardening X^{μ} are written as:

$$\begin{aligned} f^{\mu} &= \left(\frac{\sigma^{\mu D}}{(1-D)} - X^{\mu D}\right)_{eq} - \sigma_f \\ \varepsilon_{ij}^{\mu} &= \varepsilon_{ij}^{\mu e} + \varepsilon_{ij}^{\mu p} \\ \varepsilon_{ij}^{\mu e} &= \frac{1+\nu}{E}\frac{\sigma_{ij}^{\mu}}{(1-D)} - \frac{\nu}{E}\frac{\sigma_{kk}^{\mu}}{(1-D)}\delta_{ij} \\ \dot{\varepsilon}_{ij}^{\mu p} &= \frac{\partial f^{\mu}}{\partial \sigma_{ij}^{\mu}}\dot{\lambda} \\ \dot{X}_{ij}^{\mu D} &= \frac{2}{3} C \dot{\varepsilon}_{ij}^{\mu p}(1-D) \end{aligned} \tag{18}$$

where $\sigma^{\mu D}$ is the deviatoric stress at the micro-scale, C is the kinematic hardening parameter.

Finally, it is possible to compute damage evolution up to failure (crack initiation, D=D_C) as a function of the macroscopic stresses for any loading at the micro-scale.

(2) Simplified model

In order to obtain the material properties for damage analysis, the simplified identification is proposed under the following hypotheses: 1) There is no coupling between damage and elasticity at macroscale. 2) The quasi-unilateral effect is not taken into account, h =1(no difference behavior in tension and compression due to micro crack closure). 3) The damage occurs with plastic deformation simultaneously. 4) The influence of damage on the effective stress at micoscale in the yield surface is neglected. 5) The critical value of damage is assumed to be D_C=1. The simplified damage evolution rate can be expressed as a function of the macro-scopic stresses [5]:

$$dD = \left[\frac{(\sigma_{eq} + k\sigma_f)^2 R_v^{\mu}}{2ES(1+k)^2(1-D)^2}\right]^{n} \frac{d\sigma_{eq}}{C(1+k)} \quad \text{if} \quad \sigma_{eq} \ge \sigma_f \tag{19}$$

where the triaxiality function is

$$R_v^{\mu} = \frac{2}{3}(1+\nu) + 3(1-2\nu)\left[\frac{\sigma_H(1+k)}{(\sigma_{eq} + k\sigma_f)}\right]^2 \tag{20}$$

and

$$k = \frac{3aE}{2C} \tag{21}$$

where σ_H is the hydrostatic stress.

(3) Identification of material parameters

Two main material parameters, damage energy strength S and exponent n for damage evolution of Eq. (14) need to be defined. The parameters (S, n) can be identified by using Eq. (23) with a set of fatigue test data [5].

By assuming R_v^{μ} is constant and integrating Eq. (19) over one cycle symmetric loading, $\pm\sigma_M$ (Fig. 7), the damage increment per cycle written as:

$$\frac{\delta D}{\delta N}=\frac{2(R_v^{\mu})^n\left[\left(\frac{\sigma_M+k\sigma_f}{1+k}\right)^{2n+1}-\sigma_f^{2n+1}\right]}{(2n+1)(2ES)^n(1-D)^{2n}C} \tag{22}$$

Integrating Eq. (22) over the whole periodical loading up to $D=D_C=1$, gives Number of failure loading cycle as,

$$N_f=\frac{(2ES)^n C}{2(R_v^{\mu})^n\left[\left(\frac{\sigma_M+k\sigma_f}{1+k}\right)^{2n+1}-\sigma_f^{2n+1}\right]} \tag{23}$$

where

$$R_v^{\mu}\approx\frac{2}{3}(1+\nu)+3(1-2\nu)\left[\frac{1+k}{3(1+k\sigma_f/\sigma_M)}\right]^2 \tag{24}$$

Two main parameters S and n can be obtained by inverse calculation of Eq. (23) under the condition that analytical results agree with fatigue test data. However, if the damage exponent n is given in advance, the damage energy strength can be identified by the explicit formula.

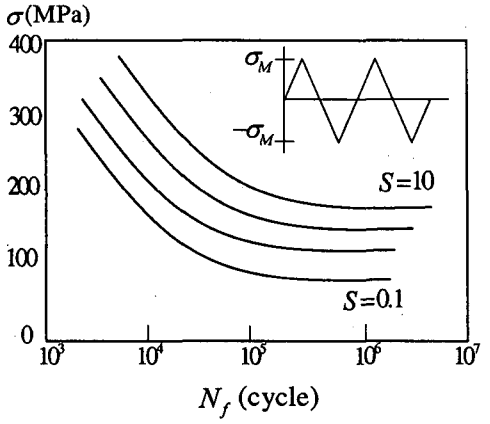

Fig. 7: S-N curve of Eq. (23)

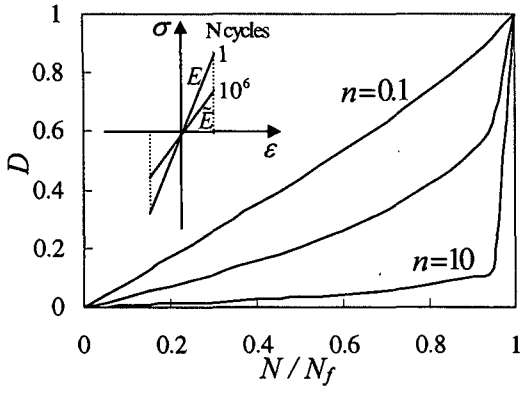

Fig. 8: damage evolution of Eq. (26)

In order to determine the damage exponent n, an additional equation is derived by substituting Eq. (23) into Eq. (22) as

$$\frac{\delta D}{\delta N}=\frac{1}{(2n+1)(1-D)^{2n}N_f} \tag{25}$$

then integrating Eq. (25) over the periodical loading to a certain number of cycle N, for damage $D < Dc$. Finally the damage is obtained as a function of normalized cycle loading:

$$D=1-\left[1-\left(\frac{N}{N_f}\right)\right]^{\frac{1}{2n+1}} \tag{26}$$

The damage exponent n can be identified by Eq. (26) with the experimental data of HCF (see Fig. 8). Where the damage value for a corresponding number of loading cycles N can be obtained by measurement of effective elastic modulus $\tilde{E}$ and substituting into $D=1-\frac{\tilde{E}}{E}$ [4]. After that, the damage energy strength S can be simply identified by Eq. (23).

2.3 Analysis Procedure

The HCF analysis procedure is shown in Fig. 9. At first, the welding residual stresses are evaluated by the inherent strain method coupling with elastic FE analysis as outlined in section 2.1. Then the residual stresses are introduced as the initial stresses into the FE-structure analysis. The initiation of a crack at macro-scale is assumed when damage reaches its critical value at any Gauss points (numerically taken D_C = 0.9 to avoid the singularity problem in Eq. (18)). Consequently, the crack area is considered implicitly to coincide with the critical damaged zone ($D=D_C$). The overall failure condition is assumed that the length of crack size reaches a certain critical value.

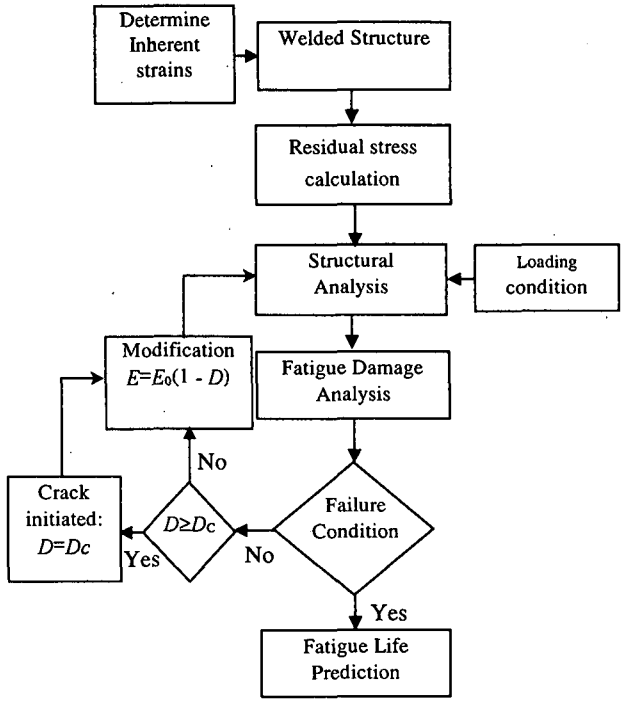

Fig. 9 HCF Analysis Procedure

3. Numerical Analysis and Results

The HCF damage analysis of a T-joint is demonstrated by the proposed method. The analytical geometry of T-joint is shown in Fig. 10. The length and thickness of model for flange and web are 600mm and 12mm, respectively. The fillet weld legs are 6mm.

The three-dimensional solid FE-mesh is selected to model a quarter of T-joint. The material data in this analysis are taken from the experiment study of Ueda and Yuan [4].

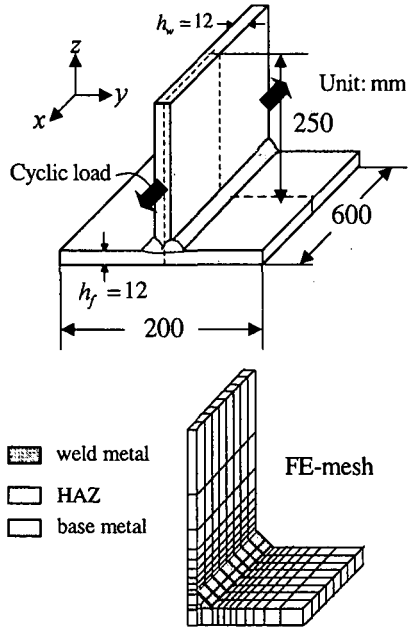

Fig. 10 Analytical model

3.1 Residual Stresses Evaluation

The welding condition of T-joint is shown in Table 1. Then the inherent strains for T-joint are evaluated by the simplified formulas in section 2.1. Then the inherent strains are introduced to 3D elastic finite element analysis to evaluate the residual stresses. From analysis results, Figs. 11(a) and 11(b) show the distribution of residual stresses in the flange and web, respectively. It is confirmed that the residual stresses that obtained by the inherent strain method agree well with the experimental results[8]. The distribution of residual stresses is not in the trapezoid due to the redistribution of stresses in FE analysis.

Table 1 Welding condition

Heat input (J/mm)	Q	2400
Melting temperature (°C)	T_m	700
Room temperature (°C)	T_0	15
Average temperature (°C)	T_{av}	90
Specific heat (J/g°C)	c	0.63
Density (g/mm^3)	ρ	7.82x10^{-3}
Thermal expansion coefficient (1/°C)	α	1.2x10^{-5}
Yield stress of weld metal & HAZ (MPa)	σ_{YW}	520
Yield stress of base metal (MPa)	σ_{YB}	330

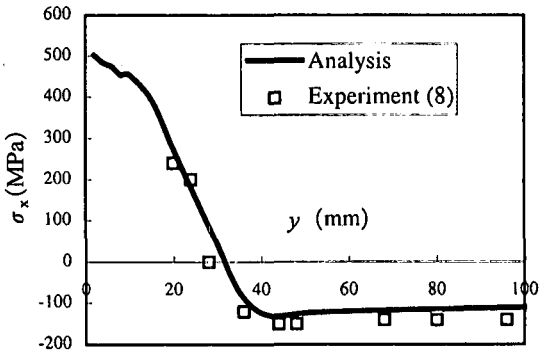

(a) flange

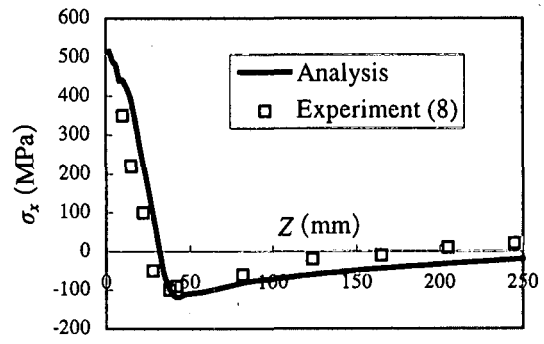

(b) web

Fig. 11 Residual stress distribution in T-joint

3.2 Fatigue Life Prediction

The HCF damage analysis and life prediction of a T-joint is performed. The T-joint is subjected to cyclic loading with constant amplitude at the location as shown in Fig. 10. The material parameters of base metal (SM400B), heat affect zone (HAZ) and weld metal are defined as in Tables 2 and 3. Two main parameters: damage energy strength S and exponent n were identified for base metal, HAZ and weld metal by the simplified model, respectively. Due to the lack of the test data that can be applied to Eq. (26), the damage exponent is simply assumed n=2 for all material same as Lemaitre's determination[5]. Under this assumption, the damage energy strength S was defined by Eq. (23) directly. The damage energy strength for base metal and weld metal are obtained S = 2.0 MPa and 6.0MPa, respectively.

Table 2 Material properties (base metal)

Elastic modulus (MPa)	E	2x10^5
Poisson's ratio	ν	0.3
Fatigue limit stress (MPa)	σ_f	160
Yield stress (MPa)	σ_y	330
Ultimate stress (MPa)	σ_u	465
Damage threshold	ε_{pD}	0.0
Critical damage	D_C	0.9
Hardening parameter (MPa)	C	470
Crack closure	h	0.2

Table 3 Material properties (weld, HAZ)

Elastic modulus (MPa)	E	$2x10^5$
Poisson's ratio	ν	0.3
Fatigue limit stress (MPa)	σ_f	220
Yield stress (MPa)	σ_y	520
Ultimate stress (MPa)	σ_u	650
Damage threshold	ε_{pD}	0.0
Critical damage	D_C	0.9
Hardening parameter (MPa)	C	500
Crack closure	h	0.2

The fatigue damage analysis is carried out until the failure condition satisfied. In this analysis, the crack area (critical damaged zone, ● as shown in Fig. 12) completely spreads through the longitudinal cross-section of T-joint, is considered to be the failure condition. Fig. 12 represents the critical damage distribution at the welded zone with respectively to number of cycle loading. The damage distribution is not uniform in the longitudinal direction x due the distribution of residual stress at the weld zone decreases from the center to the edge of T-joint as shown in Fig.13.

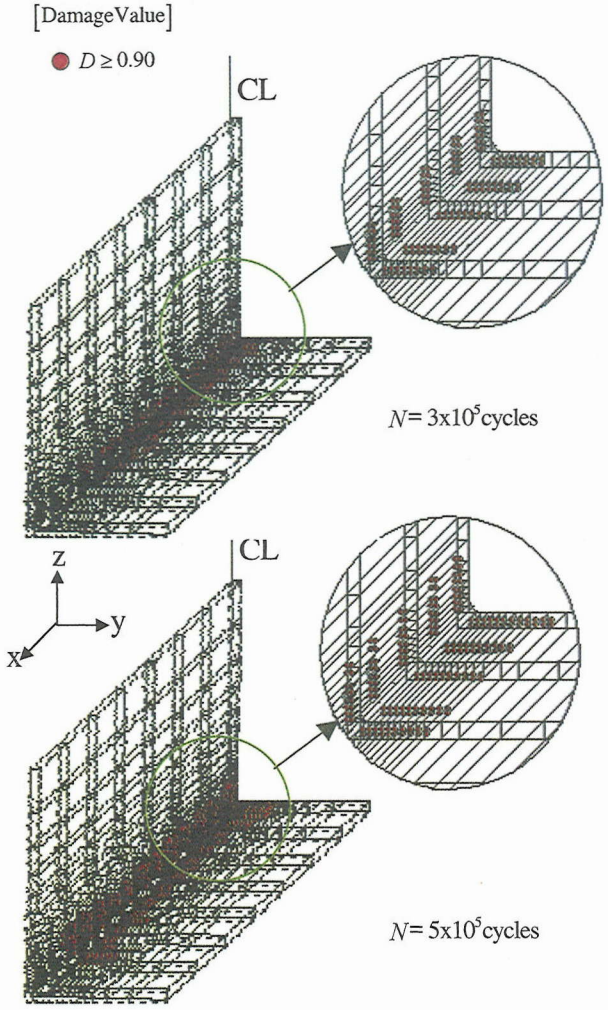

Fig. 12 Damage distribution

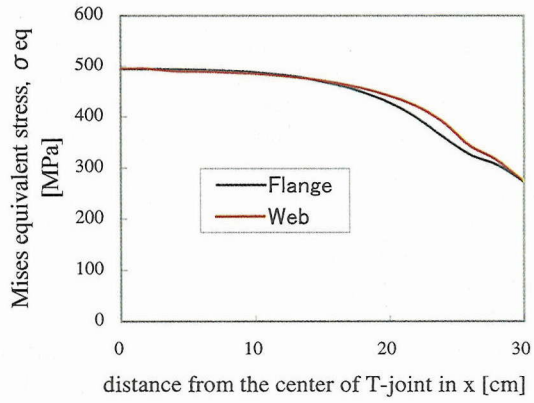

Fig. 13 distribution of residual stress at weld zone

From the analysis results, the damage evolution at the welded zone is shown in Fig. 14. The damage growth is slower with decreasing applied stress range, respectively from $\Delta\sigma$=200Mpa to 100MPa. Fig.15 shows the results of fatigue life prediction compared with the experimental results from JSSC[11]. It is observed that the proposed method can predict the accurate lifetime. Therefore, the proposed method can simulate the HCF damage behavior of the typical welded structure.

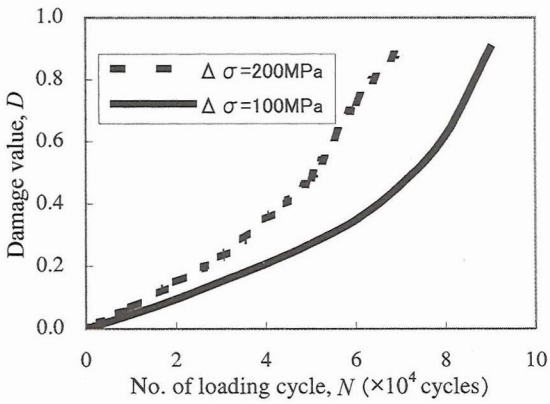

Fig. 14 Damage evolution

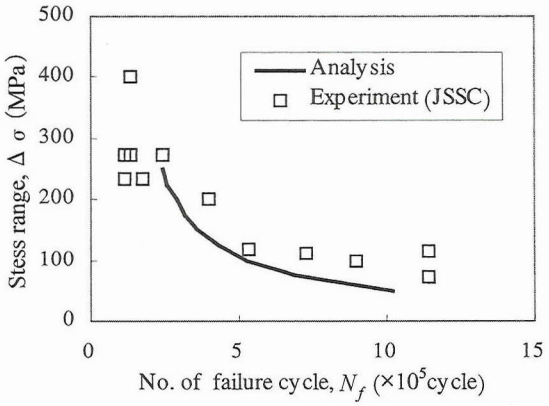

Fig. 15 Fatigue life prediction

4. Conclusions

The high cycle fatigue damage analysis based on the continuum damage mechanics was performed. The influence of the residual stresses on the fatigue damage behavior of T-joint was considered. The residual stresses were evaluated by the inherent strain method. For high cycle fatigue, a two-scale damage model is applied to evaluate the damage evolution. As it is difficult to obtain the damage parameters at the micro-scale, the identification of material parameters is proposed by using the simplified model.

From the analytical results, good agreement between the fatigue life prediction of T-joint and experimental data was confirmed. Therefore, the high cycle fatigue damage analysis and life prediction of typical welded structure under constant amplitude loading could be simulated by the proposed method. In order to obtain the reliable fatigue life for the practical application, the identification method of material properties needs to be improved. The further investigation on fatigue behavior under variable amplitude loading and definition of failure condition will be studied in the near future.

References

1) Ohta, K. and Fukazawa, M., *Bridge and Steel*, Kensetu Tosho, 2000.
2) Fisher, J.W., *Fatigue and Fracture in Steel Bridge*, John Wiley, 1984.
3) Anderson, T.L., *Fracture mechanics*, CRC Press, 1995.
4) Lemaite, J., *A Course on Damage Mechanics*, Springer Verlag, 1992.
5) Lemaite, J., Sermage, J.R. and Desmorat, R., A two-scale damage concept applied to fatigue, *International Journal of Fracture*, Vol. 97, pp.67-81, 1999.
6) Gurney, T.R., *Fatigue of Welded Structures*, Cambridge University Press, 1979.
7) Ueda, Y. & Yuan, M.G., Prediction of residual stresses in butt welded plates using inherent strains, *Journal of Engineering Materials and Technology*, Vol.115, pp.417-423, 1993.
8) Yuan, M.G. & Ueda, Y., Prediction of residual stresses in welded T- and I-joints using inherent strains, *Journal of Engineering Materials and Technology*, Vol.118, pp.417-423, 1996.
9) Kröner, E., On the plastic deformation of polycrystals, *Acta Metallurgica*,Vol.9, pp.155-161, 1961.
10) Eshelby, J.D., The determination of the elastic field of an ellipsoidal inclusion, and related problems, *Proc. of the Royal Society of London A*, Vol.241, pp. 376-390, 1957.
11) JSSC, *Fatigue design recommendations for steel structures*, Japanese Society of Steel Construction, 1995.

(Received April 18,2003)